

Atomic structure of Al/Al interface formed by surface activated bonding

T. AKATSU*, N. HOSODA, T. SUGA

Research Center for Advanced Science Technology, University of Tokyo, Japan

M. RÜHLE

Max-Planck-Institut für Metallforschung, Stuttgart, Germany

E-mail: akatsu@mpi-halle.de

Single crystalline Al crystals were bonded via surface activated bonding at room temperature with the crystallographic orientation of (111)|| (111) and [110]|| [110]. The interfacial microstructure was investigated by high-resolution transmission electron microscopy (TEM) to investigate the process of the interface formation of the system. The interface was found to form first between the tops of the protrusions which existed on the Al surfaces as roughness before bonding. At those formed bonded regions, no intermediate and damage layer was observed in the lattice images. It means that the fast atom beam irradiation used for surface activation of the metal surfaces does not alter the surface crystallinity as far as TEM observation allows. The bonded regions, however, exhibited a different contour from what could be conjectured without taking atomic rearrangement into consideration. This change in the geometrical configuration indicates that the protrusions had deformed during the bonding procedure. Microscopically, however, no disordering of the lattice was seen near the interface. Therefore, it is concluded that the heads of the protrusions have deformed plastically and then rearrangement of the atoms took place. Moreover, the defects found at the interface exhibit a delocalized core structure, indicating that the interface should have a relaxed structure. © 1999 Kluwer Academic Publishers

1. Introduction

Surface Activated Bonding (SAB) has been developed as a new technology for joining of similar and dissimilar materials without any heating process at room temperature [1, 2]. The idea is based on the fact that an attractive force will be applied on atomically clean surfaces in contact with each other. The method is very simple; the samples are brought into a vacuum chamber and cleaned or “activated” by irradiation means such as Ar fast atom beam (FAB), which is a neutralized energetic Ar beam and used most often practically, and H radical beam [3].

SAB has been shown to enable it to bond many combinations of similar and dissimilar materials such as metals, ceramics, and semiconductors. Among all the materials bonded, it is Al which has been chosen most often for one or the both of the bonding pairs. SAB of Al at room temperature has already been in use for industrial productions [4]. Al possesses suitable characteristics for SAB process. First, a very stable oxide forms on the Al surface. In other words, an active Al surface can be obtained by removing the surface oxide. Al is a material which exhibits a high elastic performance with its Young’s modulus of 68.3 GPa. It is therefore believed that the surface atoms can form bondings with

atoms on the other surface to be bonded to by adjusting their positions elastically without breaking the original bondings. The high plastic deformation performance of Al also allows to promote large area bonding with the non-heating condition in the practical cases.

Al/Al interface via SAB was once investigated [5, 6]. Those reports revealed the effect of the bonding atmosphere on the microstructure and the strength of the interface. Yet some problems remained. In those investigations, intermediate layers were found, which was interpreted as an oxide or hydroxide layer which had formed due to the reoxidation of the surface before joining in a non-UHV condition. Therefore, as a comparison, a similar interface was fabricated in another UHV machine, where, however, an Ar⁺ ion beam was used instead of the neutral Ar beam used for most SAB experiments, and its incident angle to the surface was different. At the interface of the latter case, a damaged region was found near the interface, being assumed to have formed due to the Ar implantation. Thus, these different bonding conditions did not allow an ideal investigation of the SAB interface formation between Al crystals.

Not only to Al has Al been bonded, but also to different materials such as Si, SiO₂ [3], SiC, Si₃N₄ [6], steel [7] and Al₂O₃ [8], and the microstructures of

* Present address: Max-Planck-Institut für Mikrostrukturphysik, Halle/Saale, Germany.

the interfaces with Al have been investigated. In fact, for all these combinations intermediate layers have been found. Although the intermediate layers found have been analyzed, uncertainties of their origins still remained.

The possible origins of the intermediate layers could be one or combinations of the damage due to the FAB irradiation, local deformation of the surface, reoxidation of the cleaned surface before bonding due to the atmosphere, and chemical reaction between the crystals after bonding.

In the present paper, the pair of surfaces to be bonded are both prepared macroscopically flat in order to avoid the deformation which occurred in the previous reports as much as possible. This also leads to an easier preparation of the TEM samples due to the homogeneity of the interface. The bonding procedure was carried out in an UHV SAB machine equipped with FAB sources, which was constructed after the previous studies. The main purpose of the present report is to investigate the interfacial microstructure and elucidate the interface formation between Al crystals via SAB at room temperature.

2. Experimental

From an ingot of aluminum single crystal of a purity of 99.999%, cubes of 5 mm³ were cut out by using back-reflection Laue method and a numerical controlled spark cutting machine. As a result, the cubes were obtained so that one surface of the cubes was parallel to the (111) planes with an accuracy within $\pm 1^\circ$.

The (111) surface was first polished using emery sheets of increasing finenesses from #400 up to #1500, and then buff-polished using alumina abrasive of increasing finenesses up to 1 μm . The sample cubes were next annealed at 753 K for 1 h under a vacuum of approximately 5×10^{-4} Pa, and finally electrolytically

polished in a 20% alcohol solution of perchloric acid. Following this treatment, the polished surface exhibited a roughness of 10 to 20 μm in depth and ca. 1 mm in “wave-length” and unavoidable rounding at the edges due to the electrolytic polishing. These roughness were, however, considered not to play an important role in the microscopic study. Fig. 1 shows an AFM micrograph of the Al surface after electrolytic polishing. This surface clearly has a roughness with a maximum height difference of about 8 nm and spatial distances of about 5 to 50 nm. The wave-like Al surface formed during the electrolytic polishing. This wave-like configuration was taken as a given condition for bonding, which was considered, in fact, to reflect a realistic case.

The bonding was conducted throughout in a UHV bonding system composed of several chambers, the construction having been explained in the reference [8]. The samples are first set into the preparation chamber of high vacuum. The surfaces to bond were sputter-cleaned by Ar fast-atom beam (FAB) emitted from a saddle field FAB source at an incident angle of 45° to the sample surface, operated at the acceleration voltage and current of 1.5 kV and 15 mA, respectively, for 10 min. It had already been confirmed by Auger emission spectroscopy (AES) that the native surface oxide is removed after this treatment [8]. Then the samples were transferred to the bonding chamber of ca. 10^{-7} Pa, where a load corresponding to 40 MPa was applied normal to the interface.

As bonded, the two crystals A and B were aligned so that

$$(111)A \parallel (111)B, [1\bar{1}0]A \parallel [\bar{1}10]B, [11\bar{2}]A \parallel [11\bar{2}]B$$

This gives a twin relationship at the interface, making it easier to find and observe the interface.

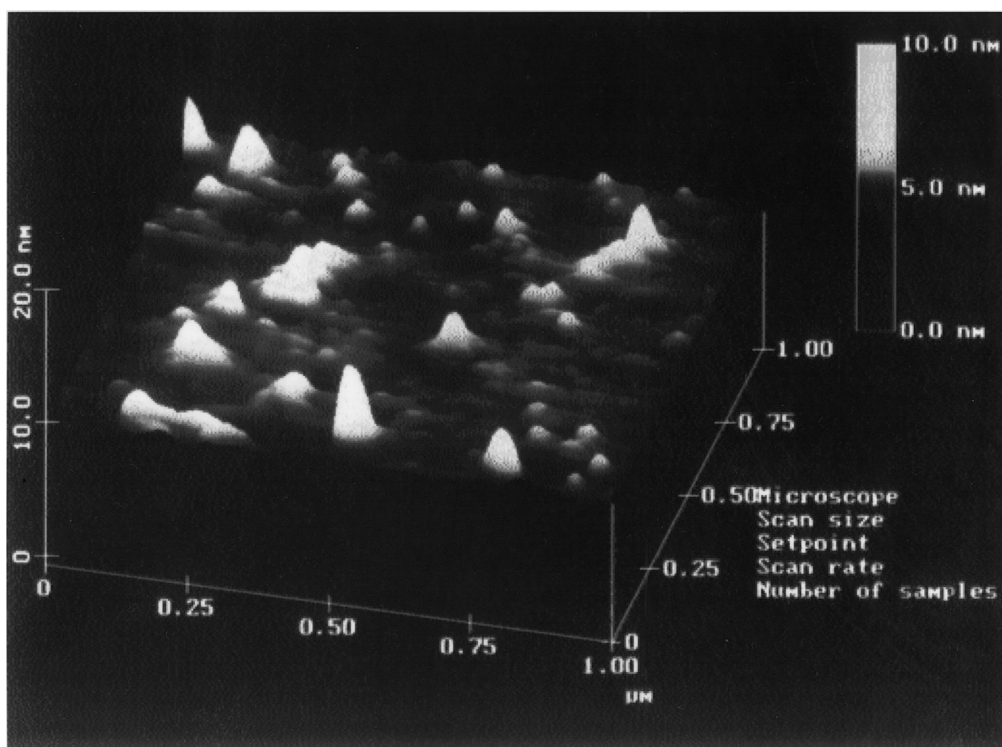


Figure 1 AFM image showing the Al surface configuration before bonding.

Cross-sectional TEM samples were prepared by electrolytically etching in an electrolyte of a 33.3% methanol solution of HNO_3 at around -25°C . At need the samples was further etched by Ar ion-thinning carefully. JEOL4000EX was operated at 400 kV, and all the TEM photographs shown in the present paper were taken in the $[1\bar{1}0]$ zone axis.

3. Results and discussion

3.1. Interface configuration

A bright field image of a typical configuration of the Al-Al interface is shown in Fig. 2. Since there were a roughness on the pre-joining surfaces of Al crystals

as mentioned above, bondings between the crystals formed at the heads of the protrusions. The gaps found between those bond regions are, therefore, non-bonding regions, where hollows on the pre-joining surfaces remained unbonded. As far as can be observed one-dimensionally in the micrographs, the proportion of bonded region is approximately 30–70%, the estimated proportion of the real bond area being 10–40%. The real applied pressure on bonded regions, therefore, can be assumed to be 100–400 MPa.

Fig. 3 is a weak-beam dark field image of another part of the interface, imaged by using (111) components of the diffraction spots. At bonded regions, dotted bright contrasts were observed, and considered

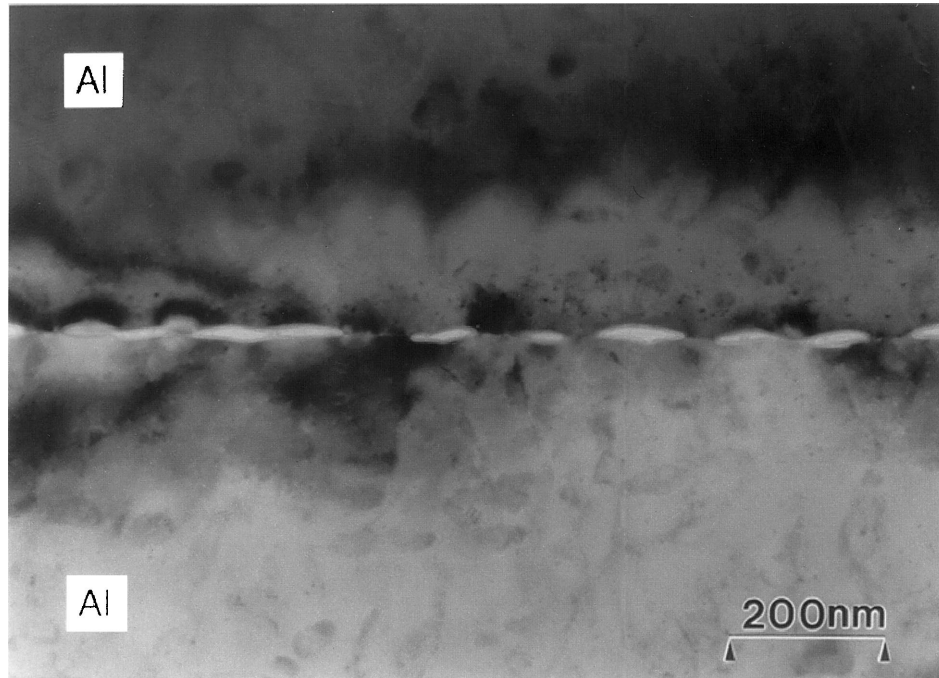


Figure 2 Interface configuration of Al/Al interface. The interface formation initiated between protrusions touching each other.

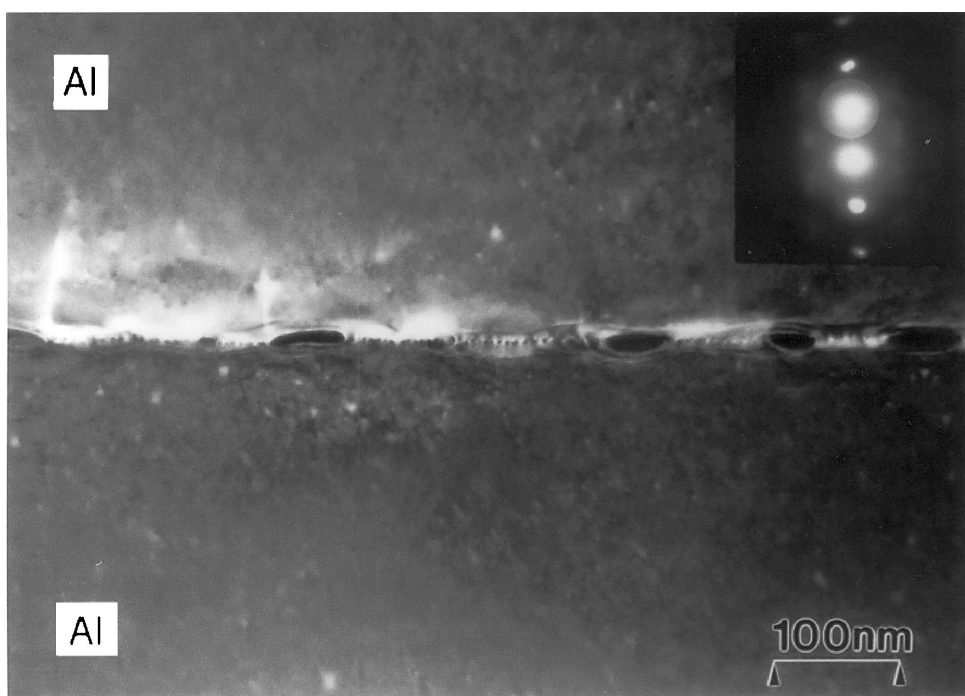


Figure 3 Weak-beam dark field image of the interface. Defects can be observed along the interface at the bonded regions.

to be the strains due to the defects formed at the interface. The structure of the defects will be discussed later. This TEM sample was prepared only by electrolytic polishing. Along the interface, a pair of contours parallel to and ca. 10 nm away from the interface on the both sides of the interface. This contour was, however, not observed along the interface in Fig. 2, which was prepared by electrolytic polishing followed by ion-thinning. Therefore, the reason for the appearance of the contours may be attributed to the electrolytic polishing of the TEM sample preparation. It is conjectured that the polishing solution should have attacked the bonded regions of higher strain than the bulk regions

as well as the gaps or unbonded regions which must have been exposed directly to the solution. Those contours disappeared by further etching the sample by ion thinning. Thus, preparation only by the electrolytic polishing may have altered the geometry and the size of the bond regions though not to a great extent. Taking this into consideration, TEM photographs shown in the following were all prepared by electrolytic polishing followed by ion-thinning shortly.

A typical feature of the bond regions is that the both edges of the bond regions display a round contour. Fig. 4 shows a bond region at a higher magnification. The edges are not sharp but blunt. If the protrusions

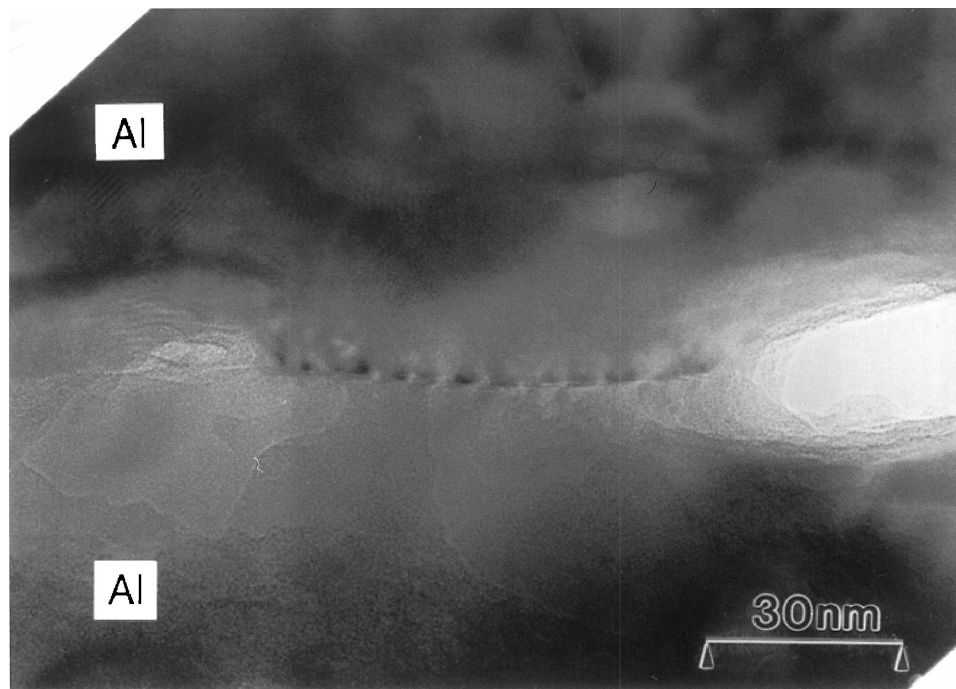


Figure 4 One of the bonded regions where two protrusions are bonded to each other. Lattice image is not disordered but the protrusions have deformed.

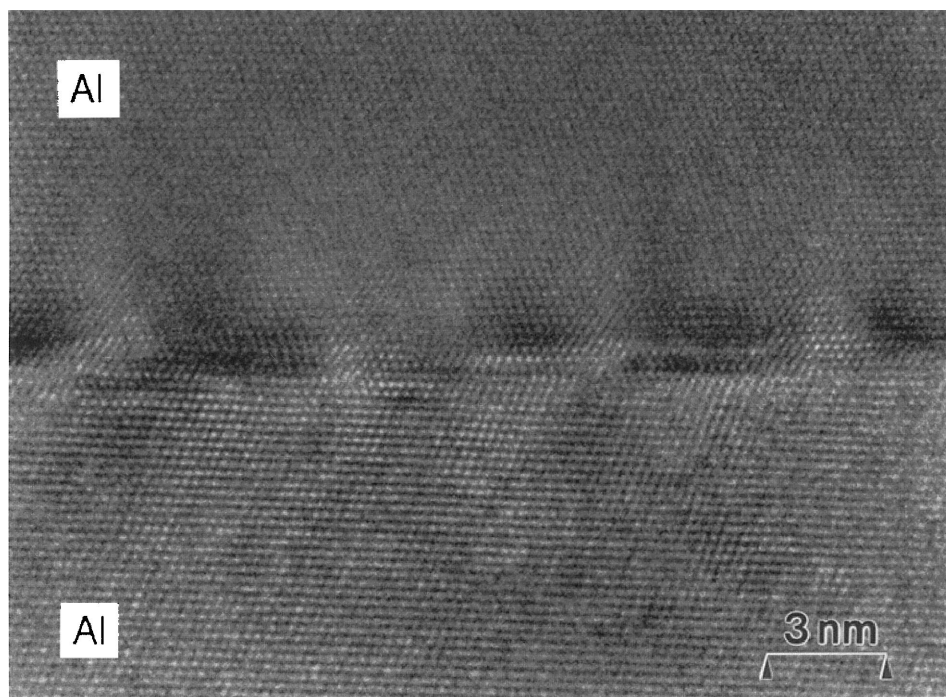


Figure 5 Lattice image of Fig. 4. An extra-plane forms at each contrast to form the interface between misoriented crystals. No oxidation layer is found.

which had existed on the pre-bonding surfaces remained touching each other by deforming only elastically, the contour would have remained sharp. This blunt structure of the bond region could form due to the tensile stress. In fact, such phenomenon has already been studied by using contact mechanics of two spheres in contact [9]. The study predicted that tensile stress exist at the edge region of such a bonded region between two substances with a curvature after reloading even though there is not any tensile stress applied from outside at all. Therefore, this blunt shape of the edges of the bond regions is considered due to this tensile stress at the edges.

Another feature of the bond regions is that the interface plane of the bond regions is flat or often bent as can be seen in Fig. 4. One side of the interface is convex and the other concave. However, the protrusions which had existed before joining must have been convex, indicating that at least one of the two sides, especially the concave side, changed its shape to from this interface. There is still a possibility that the lower side of the interface also may have changed its shape. It can be assumed on the formation of the interface under discussion as following; The lower side had a larger curvature than the upper side. As the two protrusions of different curvatures were touched and pressed to each other, the larger curvature side pushed the other side and remained its convex feature, where as the lower curvature side underwent larger deformation. Thus, as for as observation allows, change in geometry of the protrusions indicates that deformation, or microscopic plastic flow, took place. The schematic of the proposed mechanism of the interface formation is shown in Fig. 5.

3.2. Atomistic structure of the bond regions

No bond regions which were observed exhibited a damage layer up to the interface. No damage layer that would be due to Ar bombardment was observed. It means that the fast atom beam irradiation of the Al surface does not alter the surface crystallinity much as for as TEM observation allows. As can be seen in Fig. 6, a magnified view of Fig. 4, the atomic structure of the bond region displays a fine lattice image. A periodical contrast change can be seen along the interface. Each contrast has formed due to a strain introduced by edge dislocations (Fig. 6). At this bond region, the angle between the (111) planes of the two sides is approximately 2.5° . This tilt angle can also be estimated from the grain boundary dislocations. There are 9 edge dislocations at this interface of a length of ca. 80 nm, corresponding to 210 times the lattice spacing of the (111) plane of Al crystal. By assuming this interface as a pure tilt boundary, Frank's relationship

$$a/d = \sin \theta \approx \theta, \quad \text{if } \theta \ll 1,$$

where θ is the angle between the two crystals, d is the distance of dislocations and a is the lattice constant, can be applied, i.e.:

$$\theta = a/d = 9/210 \approx 2.46^\circ$$

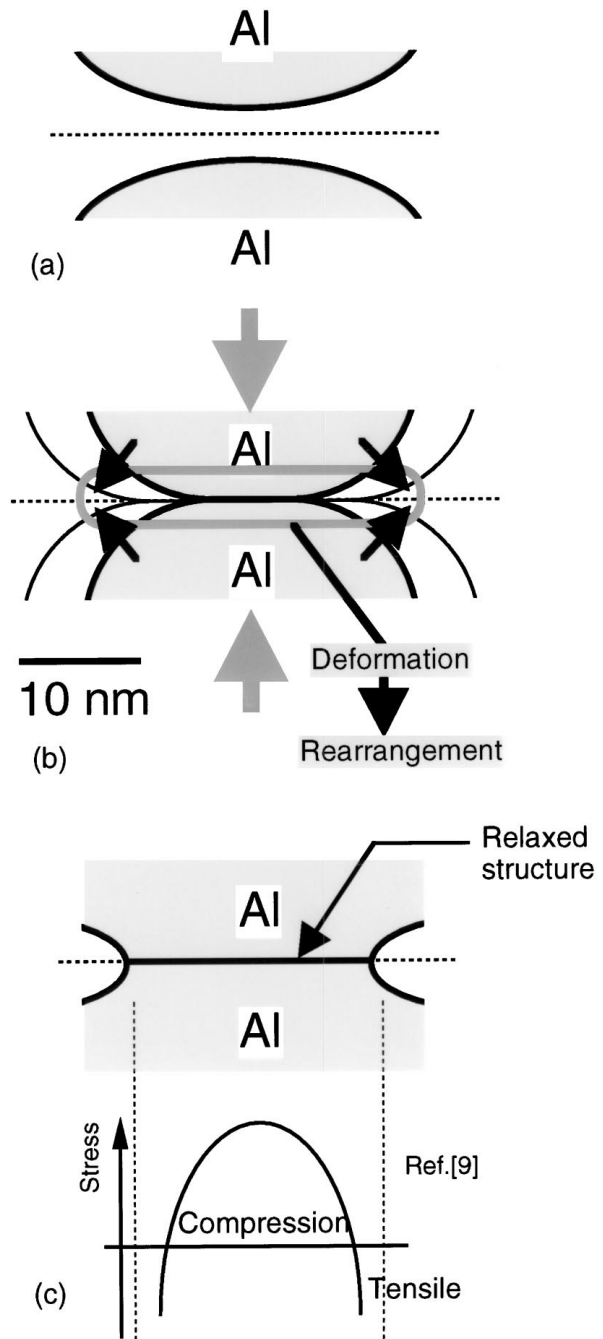


Figure 6 Expected mechanism of the Al/Al interface formation; (a) before contact, (b) contact accompanied with deformation and rearrangement of the crystals, and (c) after unloading.

This value is almost the same as that measured directly from the micrograph, 2.5° . Thus, the misorientation at the interface between the two sides led to the formation of such low-angle grain boundary dislocations.

As was mentioned above, some interfaces have a relatively flat interface plane. At those flat interface planes, atomistic structure can be observed more clearly. Fig. 7 shows a micrograph taken at such a bond region, where the tilt angle between the (111) planes of the two crystals is ca. 1.0° , which is smaller than the case discussed above. Here the interface plane can be determined precisely since a clear lattice is obtained due to the small tilt angle.

Here are edge dislocations found near the interface. The distance between the dislocations is ca. 10 nm,

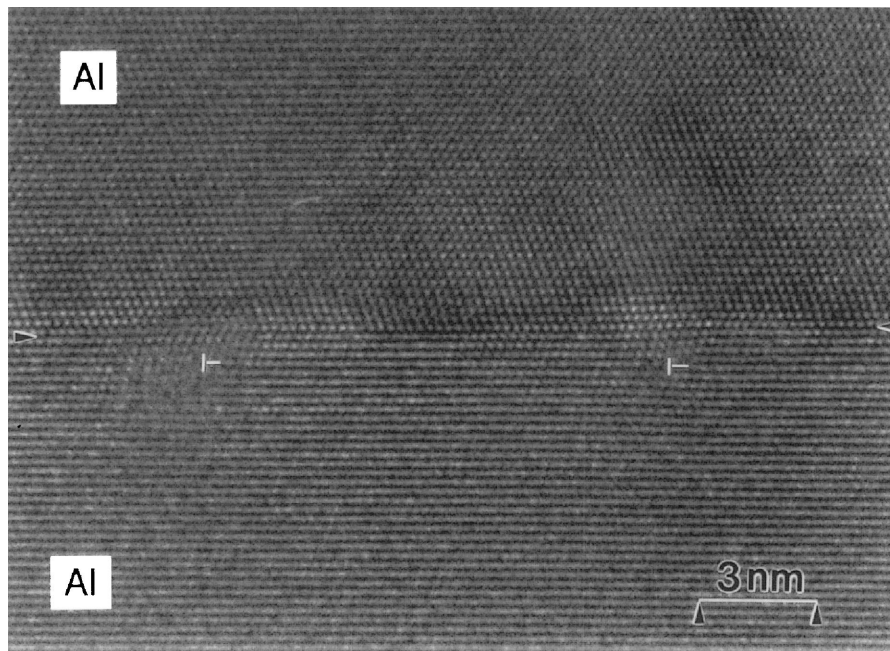


Figure 7 Lattice image of the interface with a tilt angle of 0.95° . Extra half-planes are located a couple of atomic planes away from the interface.

which is smaller than that can be estimated by Frank's relationship:

$$d \approx a/\theta = 0.4 \text{ nm}/1^\circ \approx 23 \text{ nm}.$$

Formation of more dislocations than the estimation may be attributed to atomic steps which could possibly have existed on the pre-joining surfaces. It is true that, as mentioned above, the interface formation must have been accompanied by plastic deformation and atomic rearrangement, and that further discussions cannot be made in details at this point. But it can still be conjectured that the dislocations which cannot be explained by Frank's formula are in part related to some defects which could already have existed on the crystal surfaces before bonding.

Another notable feature is that the dislocations do not perfectly lie on the interface plane, and exist a few atomic planes away from the interface. The original Al surface is not considered to have been the plane on which the two dislocations exist in the micrograph. In this case, the atoms between the plane on which the dislocations exist and the $\Sigma 3$ (111) plane should have changed its atomic positions of the upper crystal to those of the lower crystal. Therefore, this would be unlikely to occur in the energetical point of view. It should be more likely that the formed interface is the $\Sigma 3$ (111) plane in the micrograph and that the defects were absorbed inside the crystal so that a good crystallographic relationship between the crystals would be achieved.

The tendency for the atoms to take a better epitaxial relationship across the interface can be seen in the region between the two dislocations in Fig. 7. At this bond region, the upper and lower crystals are slightly in the twist relationship. The micrograph was taken in the $[1\bar{1}0]$ zone axis of the lower crystal, resulting that only (111) planes were imaged on the upper side. Nevertheless, it can be seen between the two dislocations in the micrograph that the atoms of the upper crystal

within a few atomic layers from the interface exhibit a two dimensional lattice fringes. This indicates that Al atoms were preferably aligned to achieve an epitaxial relationship between the crystals.

Fig. 8 is a magnified view of the region showing a good matching in Fig. 7. This interface displays an irregularity in the middle of Fig. 8, where the interface plane adopts a step of one (111) atomic layer. A Frank dislocation circuit applied to the defect indicates an in-plane closure failure of $1/6 [112]$. Actually, an extra atomic half-plane of (112) can be confirmed. The existence of this delocalized dislocation core is considered to be a relaxed structure of the interface. In fact, the same type of delocalized dislocation core was found at a $\Sigma = 3$, $[\bar{1}\bar{1}0]$ - $(\bar{1}\bar{1}1)$ grain boundary of Al by Shamzuzzoha *et al.* [10]. They carried out high-resolution microscopic studies on a several kinds of relaxed structures of the $\Sigma = 3$, $[\bar{1}\bar{1}0]$ - $(\bar{1}\bar{1}1)$ grain boundary structures of Al, which had undergone a mechanical deformation followed by annealing. Therefore, it is conjectured that, even in the bonding procedure of SAB at room temperature, a relaxation took place.

4. Conclusion

The Al/Al interface via SAB has been investigated and its interface formation has been discussed.

No intermediate and damage layer was observed in the lattice images at the bond regions. It means that the fast atom beam irradiation of the Al surface does not alter the surface crystallinity much as for as TEM observation allows. Change in the geometrical configuration indicates that the protrusions had deformed during the bonding procedure. Microscopically, however, no disordering of the lattice was seen near the interface. Therefore, it is concluded that the heads of the protrusions have deformed plastically and then rearrangement of the atoms took place. Thus, during the interface

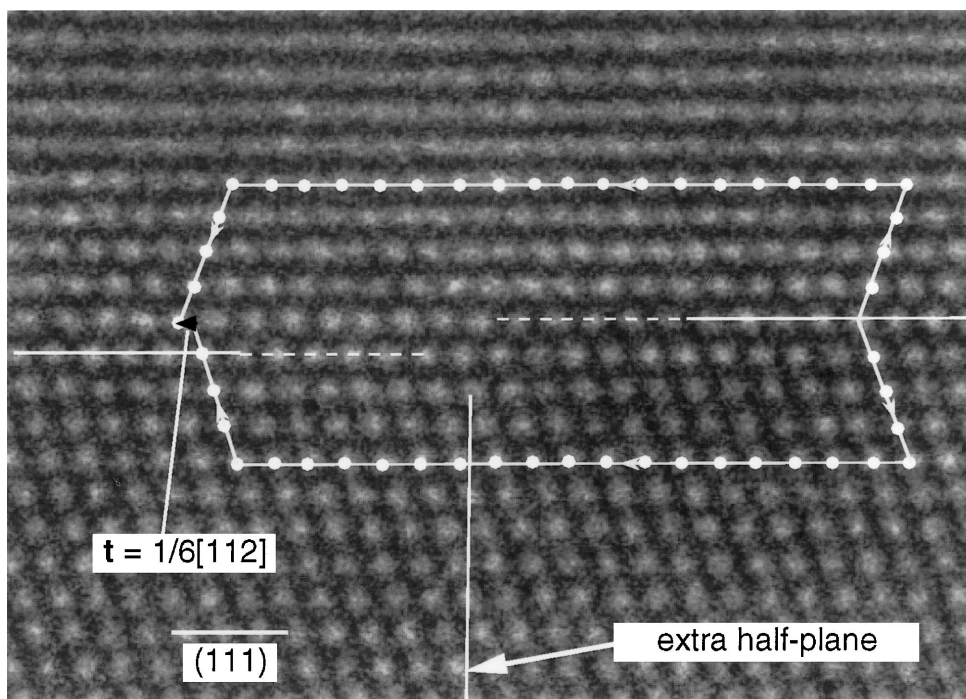


Figure 8 Magnified view of the regions between dislocations in Fig. 7. A step corresponding to one (111) spacing and the related dislocation are delocalized.

formation between Al/Al via SAB, the re-arrangement of the atoms and the relaxation of the atomic structure around the interface even at room temperature.

Acknowledgement

One of the authors (T.A.) thanks JSPS (Japanese Science Promotion Society) for the financial support.

References

1. T. SUGA, K. MIYAZAWA and Y. YAMAGATA, MRS Int. Meeting on Advanced Materials, Vol. 8, edited by N. Iwamoto and T. Suga, p. 257.
2. T. SUGA and K. MIYAZAWA, Acta/Scripta Metallurgica Proc. Series, Vol. 30, edited by M. Rühle, A. G. Evans, M. F. Ashy and J. P. Hirth, 1990, p. 189.
3. N. HOSODA, Y. KYOGOKU and T. SUGA, *J. Mater. Sci.* **33** (1998) 253–258.
4. Toyo-Kohan Technical Report, Toyo-Kohan Co. Ltd, 1995.
5. T. SUGA, Y. TAKAHASHI, H. TAKAGI, Y. ISHIDA, G. ELSSNER, B. GIBBESCH and Y. BANDO, *J. Japan Inst. Metals* **4**(6) (1990) 741–742.
6. T. SUGA, Y. TAKAHASHI, H. TAKAGI, Y. ISHIDA, G. GIBBESCH and G. ELSSNER, *Acta Metall. Mater.* **40**(Suppl.) (1992) S133–S137.
7. L. YANG, N. HOSODA and T. SUGA, *Interface Science* **5** (1997) 279–286.
8. T. AKATSU, G. SASAKI, H. HOSODA and T. SUGA, *J. Mater. Res.* **12**(3) (1997) 852–856.
9. K. L. JOHNSON *et al.*, *Proc. Roy Soc., London* **A324** (1971) 301–313.
10. M. SHAMZUZZOHA, P. A. DEYMIER and D. J. SMITH, *Phil. Mag. A* **64**(1) (1991) 245–253.

Received 8 December 1998
and accepted 15 March 1999